Multiphase Multidimensional Simulation of Geothermal Reservoirs

T. J. LASSETER

Geonuclear Nobel Paso, Paris, France; currently with Intercomp Inc., The Hague, The Netherlands

P. A. WITHERSPOON

M. J. LIPPMANN

Lawrence Berkeley Laboratory and Department of Civil Engineering, University of California, Berkeley, California 94720, USA

ABSTRACT

A mathematical method of modeling geothermal reservoirs has been developed using a computer program called SHAFT (Simultaneous Heat and Fluid Transport). This program numerically solves the coupled equations describing the simultaneous transport of mass and energy by a one- or two-phase fluid in porous media for transient or steady-state systems in one, two, or three dimensions. The governing equations are set up in terms of two expressions, one for flow and one for internal energy. Solutions are obtained by solving for two unknowns, density and internal energy, as a function of time and position within the system. Details of the development of flow and energy equations are presented. Two examples of the application of SHAFT to two-phase geothermal reservoirs are included.

INTRODUCTION

Geothermal systems are receiving an increasing amount of attention, and consequently it is important to understand the behavior of these complex systems. One approach is to simulate their behavior by use of mathematical models, and a recent review (Witherspoon et al., 1975) reveals the growing interest in such methods. As part of our research effort in this field we have developed a computer program called SHAFT, which stands for simultaneous heat and fluid transport. This program is an extension of an earlier code developed by Lasseter and Witherspoon (1974) to handle nonisothermal flow of gases in porous media.

SHAFT numerically solves the coupled equations describing the simultaneous transport of mass and energy by a one- or two-phase fluid in porous media for transient or steady-state systems in one, two, or three dimensions. The fluid must be pure or of uniform composition in both phases, although different fluids can be handled as long as they are confined to separate regions of the system. The equation of state which describes the thermodynamic behavior of the fluid is a function not only of the fluid's inherent properties but also of the position of the fluid within the system. This is particularly important for flow in porous media where interactions between the fluid and solid matrix mean that the thermodynamic behavior of the fluid is dependent on the nature of the matrix as well as of the fluid.

GENERAL APPROACH

The classical behavior of matter can be fully described in terms of three equations for the conservation of mass, momentum, and energy. For a multicomponent fluid, we must have a conservation-of-mass equation for each component, but in the present approach we have assumed that the fluid is pure water. We therefore have only one equation for conservation of mass. This approach may also be applicable to mixtures whose composition is essentially the same in both liquid and vapor phases.

For flow in porous media, it is customary to describe the behavior of the system on a macroscopic scale and to replace the momentum equation by the empirical equation known as Darcy's Law. Darcy (1856) determined that the flow of water through a bed of sand was proportional to the pressure gradient. His law has since been extended to other fluids in many different kinds of porous and fractured media. Deviations from Darcy behavior have also been observed, but in most practical field problems Darcy's law is perfectly acceptable. Since we shall be dealing with two-phase flow, we must have separate Darcy equations for each phase.

Thus, the basic governing equations in the present version of SHAFT consist of one equation for conservation of mass, two Darcy equations, and one energy equation. We will show how the conservation-of-mass equation and the two Darcy equations can be combined into a single equation, which will be called the "flow" equation. The resulting flow and energy equations can be solved numerically for two unknowns, the density and internal energy of the fluid as a function of time and position within the system.

The most rigorously correct procedure is to solve these two equations in a completely coupled manner. To do this, one would estimate the energy field and solve for the density distribution at a particular time. By substituting the density distribution back into the energy equation, one could obtain

a better estimate of the energy field, which could then be used in the flow equation to obtain a second solution for the density distribution. This process could be continued until the differences between successive estimates of the energy and density distributions are within acceptable limits. This procedure would have to be repeated for each time step and becomes expensive and time-consuming for large problems.

Direct methods of solving the coupled flow and energy equations are also possible. However, the nonlinearities in the equations and the large differences in time constants between the two governing equations make such a technique less efficient than the one we use.

The SHAFT program uses a standard technique that has been found acceptable in many applications and involves decoupling the governing equations. In this method, one starts with the initial energy distribution and assumes that this distribution remains relatively constant over a short interval of time. We then solve for the new density distribution at the end of the time step. Using this new density distribution, we solve for the energy field at the end of a second time interval, and so on.

What makes this approach possible is that the energy field varies much more slowly than the density field, that is the energy time constants of the system are much larger than the corresponding density time constants. Thus, while it is necessary to take relatively small time steps to accurately solve the density equation, the energy field time steps can be much larger. Selecting the appropriate time steps so that the solution procedure is both accurate and efficient is one of the most important parts of this numerical method.

Basic Numerical Method

The basic numerical method can be most easily demonstrated by developing the finite difference equation for the simple transient conductive heat flow equation:

$$pc\frac{\partial T}{\partial t} = \nabla \cdot k\nabla T \tag{1}$$

where ρ is the density of the material, c is the heat capacity, T is the temperature, t is time, and k is the thermal conductivity (see Table 1 for a complete nomenclature list).

Integrating Equation (1) over a region R having a volume V and a surface S having an area A, and applying the divergence theorem to the right-hand side, we have:

$$\int_R \left(\rho c\frac{\partial T}{\partial t}\right) dv = \oint_S (k\nabla T \cdot \hat{n})\, da \tag{2}$$

where $\hat{n}$ is the outward-directed unit normal to the surface S.

To derive the corresponding finite difference equation, we will make the following assumptions: (1) the volume integral on the left-hand side can be represented by an average value times the volume of region R; and (2) the surface S of the region can be broken into a series of subsections, A_m, over which the normal component of the conductive energy flux vector can be approximated with an average value.

We can therefore rewrite Equation (2) as

$$V\left(\rho c\frac{\partial T}{\partial t}\right) = \sum_m A_m k_m (\nabla T)_m \tag{3}$$

where k_m is the effective thermal conductivity over surface subsection m and $(\nabla T)_m$ is the normal component of the temperature gradient vector over the surface subsection m. We will now consider a general region which we have subdivided into many subregions. We will refer to these subregions as nodes. Figure 1 shows a typical node n connected to an adjacent node m. The area of the interface between these nodes is denoted as $A_{n,m}$. The distance $d_{n,m}$ between nodal point n and the interface between nodes n and m is measured along a line perpendicular to that surface (Fig. 1). The numerical method used as well as the algorithm developed for the program are such that node n can be connected to any number of nodes desired by the user.

Equation (3) can be immediately applied to the solution of the energy balance for node n once we have defined the normal component of the temperature gradient vector and the effective conductivity over the surface subsection m.

Determining the normal component of the temperature gradient vector would be conceptually easy if we had some idea of the temperature variation within the nodes. Since the temperature distribution within the nodes is represented only by an average value, this is not possible. We therefore assume that the normal component of the temperature gradient vector is equal to the temperature difference between the nodes divided by the distance between the geometric centers of the nodes (or some other distance if more appropriate), where we define the distance as the sum of the two normal distances from the geometric centers of the nodes to the interface. While this may seem a gross simplification, it is clear that as the nodes become smaller and smaller, this approximation approaches the mathematically correct solution. The advantage of this approach is the fact that the numerical method used in solving the system of equations of this form is very fast and can solve systems containing a large number of nodes.

To solve this equation numerically, we must also replace

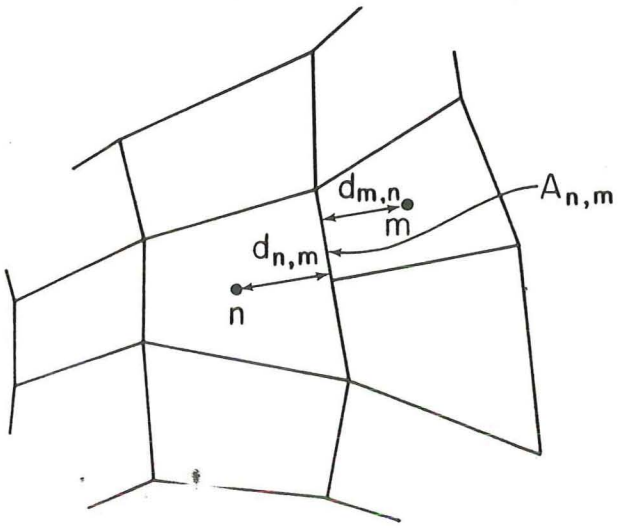

Figure 1. Typical node connection network and nomenclature.

Table 1. Nomenclature. Dimensions are mass (M), length (L), time (t), and temperature (T).

Symbol	Meaning	Dimensions
A	area	L^2
c	specific heat at constant volume	$L^2\,t^{-2}\,T^{-1}$
C	heat capacity	$ML^2\,t^{-2}\,T^{-1}$
$d_{n,m}$	distance between nodal point n and interface between nodes n and m	L
$D_{n,m}$	distance between nodal points n and m ($D_{n,m} = d_{n,m} + d_{m,n}$)	L
E	specific (internal) energy	$L^2\,t^{-2}$
f	fraction of net mass flux rate which is vapor	–
F	mass flux	$M\,t^{-1}$
g	acceleration parameter ($g > 0$)	–
$\mathbf{g}$	acceleration due to gravity	$L\,t^{-2}$
k	thermal (or effective thermal) conductivity	$ML\,t^{-3}\,T^{-1}$
K	intrinsic permeability	L^2
m	mass	M
M	mobility	$M^{-1}\,L^3\,t$
$\hat{n}$	outward directed normal to surface	–
P	fluid pressure	$M\,L^{-1}\,t^{-2}$
q	energy flux across surface	$ML^2\,t^{-3}$
Q	energy injection rate from sources within node (or volume V)	$ML^2\,t^{-3}$
R	relative permeability	–
S	mass injection rate per unit volume from sources within node (or volume V)	$ML^{-3}\,t^{-1}$
t	time	t
T	temperature	T
$\bar{T}$	average temperature	T
$\mathbf{v}$	Darcy fluid velocity	$L\,t^{-1}$
V	volume	L^3
Z	sum of transductances	$ML^2\,t^{-3}\,T^{-1}$
$\beta_{n,m}$	direction cosine between the normal from node n to m and the gravitational acceleration vector	–
ϵ	energy content of volume V	$ML^2\,t^{-2}$
θ	interpolation factor ($0.5 \leq \theta \leq 1.0$)	–
λ	weighting factor ($0.5 \leq \lambda \leq 1.0$)	–
μ	viscosity	$ML^{-1}\,t^{-1}$
ρ	density	ML^{-3}
ϕ	porosity	–
Ω	transductance	$ML^2\,t^{-3}\,T^{-1}$
$(\nabla T)_m$	normal component of the temperature gradient vector over the surface subsection m	TL^{-1}
$(\,)^*$	lumped parameter	arbitrary
Subscripts		
c	convective	
down	at downstream node	
e	fluid-solid mixture	
ex	explicit	
f	fluid	
l	liquid	
m	at node (or surface subsection) m	
n	at node (or time step) n	
n,m	at interface between nodes n and m	
s	solid	
up	at upstream node	
v	vapor	
Superscripts		
a	at surface A	
l	liquid	
p	iteration number	
v	vapor	

the infinitely small time change ∂t with a finite time change or time-step Δt. We can now write the difference equation form of Equation (3):

$$V_n \rho_n c_n \frac{\Delta T_n}{\Delta t} = \sum_m \frac{A_{n,m} k_{n,m}}{D_{n,m}} (\bar{T}_m - \bar{T}_n) \qquad (4)$$

Here we have put a bar over T_m and T_n because, for the maximum accuracy, they must be values of the temperatures between those at the beginning and at the end of the time step. If we know the exact form of the temperature change during the time step, this intermediate value can be selected so that it exactly equals the time integrated average of the temperature over the time step. If this could be done with complete accuracy, absolutely no error would be introduced by the time step procedure. Unfortunately, however, we can only estimate what the form of the temperature change is. But for sufficiently small time steps, little error should be introduced. One of the important sophistications of the numerical procedure used is the manner in which it estimates the average temperature for the time step. The average temperature for each node, then, can be written as

$$\bar{T}_n = T_n + \theta \Delta T_n \qquad (5)$$

where T_n is the temperature at the beginning of the time step, ΔT_n is the change in temperature during the time step, and θ is a value between 0.5 and 1.0. The value of θ is determined every time step and is the same for all nodes for that time step.

We also have the problem of defining the effective thermal conductivity, $k_{n,m}$. Without going into detail, it can be shown (Lasseter and Witherspoon, 1974) that continuity of temperature and energy flux is maintained at the interface if the effective conductivity is written in terms of the conductivities of the material in each node as

$$\frac{D_{n,m}}{k_{n,m}} = \frac{d_{n,m}}{k_n} + \frac{d_{m,n}}{k_m} \tag{6}$$

where

$$D_{n,m} = d_{n,m} + d_{m,n}.$$

We can now rewrite Equation (4) as

$$V_n \rho_n c_n \frac{\Delta T_n}{\Delta t} = \sum_m \frac{A_{n,m} k_{n,m}}{D_{n,m}} [(T_m - T_n) + \theta (\Delta T_m - \Delta T_n)]. \tag{7}$$

The first term in the brackets of Equation (7) is the "explicit" part, since these values are known at the beginning of the time step. The second term is the "implicit" part since it contains the temperature changes for which we are solving.

For a system of n nodes, we have a system of n equations like Equation (7) to solve. The SHAFT program, like the TRUMP program on which it is based (Edwards, 1972), uses an iterative technique to solve these equations. We first rewrite Equation (7) for simplicity as

$$\Delta T_n = \Delta T_{n,ex} + \frac{\theta \Delta t}{C_n} \sum_m \Omega_{n,m} (\Delta T_m - \Delta T_n) \tag{8}$$

where

$$C_n = \rho_n c_n V_n$$

$$\Delta T_{n,ex} = \frac{\Delta t}{C_n} \sum_m \Omega_{n,m} \{T_m - T_n\}$$

$$\Omega_{n,m} = A_{n,m} k_{n,m} / D_{n,m}.$$

Defining $Z_n = \Sigma_m \Omega_{n,m}$, we can solve Equation (8) for ΔT_n:

$$\Delta T_n = \frac{\Delta T_{n,ex} + \frac{\theta \Delta t}{C_n} \sum_m \Omega_{n,m} \Delta T_m}{1 + \frac{\theta \Delta t}{C_n} Z_n} \tag{9}$$

This iterative procedure was first derived by Evans Brousseau, and Keirstead (1954) and is called an acceleration method; it is similar to, but different from, the successive over-relaxation method often used. To implement this technique, we substitute in the left side of Equation (8) $\Delta T_n = \Delta T_n^{(p+1)}$, and in the right side we substitute $\Delta T_n = (1 + g) \Delta T_n^{(p+1)} - g \Delta T_n^{(p)}$ and $\Delta T_m = \Delta T_m^{(p)}$, where g is the acceleration parameter ($g > 0$), and p is the iteration number in the superscript. Making these substitutions, Equation (8) can be rewritten:

$$\Delta T_n^{(p+1)} = \Delta T_{n,ex} + \frac{\theta \Delta t}{C_n} \left(\sum_m \Omega_{n,m} \Delta T_m^{(p)} - (1 + g) Z_n \Delta T_n^{(p+1)} + g Z_n \Delta T_n^{(p)} \right). \tag{10}$$

We can then solve Equation (10) for ΔT_n at the $p + 1$ iteration in terms of ΔT_n and ΔT_m at the p iteration:

$$\Delta T_n^{(p+1)} = \frac{\Delta T_{n,ex} + \frac{\theta \Delta t}{C_n} \left(\sum_m \Omega_{n,m} \Delta T_m^{(p)} + g Z_n \Delta T_n^{(p)} \right)}{1 + (1 + g) \frac{\theta \Delta t}{C_n} Z_n}. \tag{11}$$

The iteration procedure would begin with an estimate of the temperature changes in each of the nodes which we will call the "zeroth" iteration. We then compute the values at the first iteration using Equation (11) and the zeroth iteration values, and so on. The iteration procedure is stopped when the maximum change in temperature between successive iterations is less than some prescribed value.

The stability and convergence for this iterative procedure are discussed by Lasseter (1975). For this difference equation as well as those to be developed describing multiphase convective heat and mass transfer, stability and convergence are guaranteed regardless of node size and shape and of the contrast in material properties between nodes.

This is the basic numerical method that will be used in solving the more complete energy and mass transport equations to be discussed in the following sections. The advantages of this method are discussed in detail by Edwards (1972) and Lasseter (1975).

The Internal Energy Equation

Numerous authors have developed the form of the internal energy equation appropriate for convective and conductive energy transport in porous media. Rather than reproduce one of these more rigorous derivations, we prefer to present a derivation which is simpler and more "physical" than most. In the succeeding discussion we will refer to the internal energy simply as energy.

The energy equation is a simple balance equation. It can best be described by considering a small volume V. The energy equation keeps track of the energy content of V and the fluxes of energy in and out of V. In words, it can be written:

[the time rate-of-change of energy in V] = [the flux of energy in and out of V] + [energy sources within V]

The corresponding mathematical equation is written:

$$\frac{\partial \epsilon}{\partial t} = -\oint_A \mathbf{q}\cdot\hat{n}\, da + Q \tag{12}$$

where ϵ is the energy content of V, $\mathbf{q}$ is the flux of energy in units of energy per unit area per unit time across the surface A of the volume V, $\hat{n}$ is the unit vector normal to A in the outward direction from V, and Q is the energy injection rate from sources within V.

For a porous medium, we will consider a volume V which contains fluid, designated by the subscript f, and solid, designated by the subscript s. Properties of the fluid-solid mixture will be designated by the subscript, e.

The energy content of the volume is then given by

$$\epsilon_e = m_f E_f + m_s E_s \tag{13}$$

where m is the mass and E is the energy per unit mass.

For convenience, we will assume that the volume V expands and contracts with the solid "skeleton" of the porous media. Thus the solid mass is always the same since no mass moves across the surface of the volume. The fluid mass will, in general, change with time as the fluid flows in and out of the volume.

The energy balance, Equation (12) can then be written:

$$E_f\frac{dm_f}{dt} + m_f\frac{dE_f}{dt} + m_s\frac{dE_s}{dt} = -\oint_A \mathbf{q}\cdot\hat{n}\, da + Q. \tag{14}$$

The energy flux, $\mathbf{q}$, consists of the conduction and convection components, which for a single-phase fluid can be written:

$$\mathbf{q} = F_f^a E_f^a - k_e^a (\nabla T)_e^a \tag{15}$$

where F_f^a is the mass flux of fluid across the surface A, k_e^a is the effective thermal conductivity of the fluid-solid matrix evaluated at A, $(\nabla T)_e^a$ is the temperature gradient in the matrix at A (we assume the fluid and solid are in thermal equilibrium), and E_f^a is the energy of the fluid crossing A.

For completeness a compressible work term (reversible conversion of internal energy to kinetic energy) and a viscous dissipation term (irreversible conversion of kinetic energy to internal energy by frictional forces at the fluid-solid interfaces) should be included in the balance equation. Even though these terms could be added to the program, at the present time, they have been neglected because it is believed these phenomena are probably not important in most geothermal reservoir systems.

We can now rewrite the first term on the left-hand side of Equation (14) as:

$$E_f\frac{dm_f}{dt} = -E_f\oint_A \mathbf{F}_f^a\cdot\hat{n}\, da + E_f S V \tag{16}$$

where S is the mass injection rate, per unit volume, from sources within V. Substituting Equations (15) and (16) into (14), we have:

$$V_f\rho_f\frac{dE_f}{dt} + m_s\frac{dE_S}{dt} = \oint_A \{E_f - E_f^a\}\,\mathbf{F}_f^a\cdot\hat{n}\, da + \oint_A k_e^a (\nabla T)_e^a\cdot\hat{n}\, da + Q - E_f S V. \tag{17}$$

Note that if the system is deforming, the volume of fluid originally within the volume V may be changing with time. Thus, V_f must be specified as a function of time, pressure, and/or temperature.

Difference Form of Energy Equation

Before writing the difference form of the energy equation, several points should be discussed. It is obvious that Equation (17) consists of several unknowns: E_f, E_s, $\mathbf{F}_f$, T_e, and ρ_f. It is assumed that the conductivity, k_e, and the source terms, Q and S, are defined. For a two-phase homogeneous fluid, one can show that the thermodynamic state of the fluid can be uniquely defined in terms of its internal energy and density. Temperature and pressure do not uniquely define the fluid state since, during phase change, these two variables may be constant while the fluid energy is changing. We could also solve the two equations in terms of internal energy and pressure, but in order to guarantee strict conservation of mass, we solve the flow equation in terms of density rather than pressure.

We will assume that the solid and fluid are in thermodynamic equilibrium; that is, in each node we assume that they are at the same temperature and pressure. Knowing the temperature of the fluid will tell us the energy of the solid. We can therefore define the solid energy as a function of the fluid energy and density. Thus we can write

$$\frac{dE_s}{dt} = \left[\left(\frac{\partial E_s}{\partial E_f}\right)_\rho + \left(\frac{\partial E_s}{\partial \rho}\right)_{E_f}\frac{d\rho}{dE_f}\right]\frac{dE_f}{dt} \tag{18}$$

We evaluate $d\rho/dE_f$ from computed values of the time derivatives:

$$\frac{d\rho}{dE_f} = \frac{d\rho/dt}{dE_f/dt}. \tag{19}$$

In deriving the difference equations, a similar situation arises in the evaluation of ΔT and ΔP in terms of our dependent variables E and ρ. We can write ΔT for example as

$$\Delta T = \left[\left(\frac{\partial T}{\partial E_f}\right)_\rho + \left(\frac{\partial T}{\partial \rho}\right)_{E_f}\frac{d\rho}{dE_f}\right]\Delta E_f = \frac{dT}{dE_f}\Delta E_f. \tag{20}$$

In deriving the finite difference form of the energy equation, we will use "upwind" differencing in the convective transport term to determine the interface energy. That is, the interface energy is not determined by a spatial interpolation of the energies of the two adjacent nodes, but is "weighted" in the direction from which the fluid crossing that interface is coming. This weighting is intuitively correct as well as being required for numerical stability. Thus the energy of the fluid at the interface between nodes n and m is written:

$$E_{n,m} = \lambda E_{\text{up}} + (1-\lambda) E_{\text{down}} \tag{21}$$

where E_{up} is the energy of the upstream node, E_{down} is

the energy of the downstream node, and λ is the weighting factor and must be between 0.5 and 1.0.

To guarantee stability, the change in the interface energy must be equal to the change in the energy of the upstream node, $\Delta E_{n,m} = \Delta E_{up}$.

With these points in mind, and dropping the subscript f, we can write the difference form of the single-phase energy equation as

$$\left(V_f\rho + m_s\frac{dE_s}{dE}\right)_n \frac{\Delta E_n}{\Delta t} \tag{22}$$

$$= \sum_m \left\{ [\lambda E_{up} + (1-\lambda)E_{down} - E_n]F_{n,m} + \frac{A_{n,m}}{D_{n,m}} k_{n,m}(T_m - T_n) \right\} + Q_n - E_n S_n V_n$$

$$+ \theta \sum_m \left[\Delta E_{up} F_{n,m} + \frac{A_{n,m}}{D_{n,m}} k_{n,m} \left(\frac{dT_m}{dE_m}\Delta E_m - \frac{dT_n}{dE_n}\Delta E_n \right) \right]$$

where E_n is the fluid energy of node n, $F_{n,m}$ is the fluid flow rate between the nodes m and n (positive if into n), $A_{n,m}$ is the area connecting nodes m and n, $D_{n,m}$ is the distance between nodal points n and m, T_n is the temperature of node n, $\rho_{n,m}$ is the density of the fluid crossing the boundary between nodes m and n, Q_n is the energy injection rate into node n, and S_n is the mass injection rate, per unit volume, into node n.

To derive the difference form of the two-phase energy equation, we need only recognize that the convective transport term in Equation (15) must be replaced by two terms describing the convective transport of liquid and vapor. Defining the convective transport term as $\mathbf{q}_c$, the two-phase convective transport term can be written:

$$\mathbf{q}_c = \mathbf{F}_v^a E_v + \mathbf{F}_l^a E_l = [E_l + (E_v - E_l)f]\,\mathbf{F}_f^a \tag{23}$$

where $\mathbf{F}_v^a$ is the mass flux rate of vapor in units of mass per unit area per unit time, $\mathbf{F}_l^a$ is the mass flux rate of liquid, E_v is the internal energy of the vapor, E_l is the internal energy of the liquid, $\mathbf{F}_f^a$ is the net mass flux rate of fluid, and f is the fraction of the net mass flux rate of fluid which is vapor.

Note that if the liquid and vapor are moving in opposite directions, the vapor fraction, f, need not be positive nor must its magnitude be less than one. The two-phase energy equation can then be written:

$$\left(V_f\rho + m_s\frac{dE_s}{dE}\right)_n \frac{\Delta E_n}{\Delta t} \tag{24}$$

$$= \sum_m \left\{ [E^l_{n,m} + (E^v_{n,m} - E^l_{n,m})f_{n,m} - E_n]F_{n,m} + \frac{A_{n,m}}{D_{n,m}} k_{n,m}(T_m - T_n) \right\} + Q_n - E_n S_n V_n$$

$$+ \theta \sum_m \left[\Delta E_{up} F_{n,m} + \frac{A_{n,m}}{D_{n,m}} k_{n,m} \left(\frac{dT_m}{dE_m}\Delta E_m - \frac{dT_n}{dE_n}\Delta E_n \right) \right].$$

Here we have approximated the change in the vapor fraction of the flux in terms of the change in the vapor fraction of the upstream node. This is only an approximation, but we feel it is acceptable for a number of reasons. First of all, the time steps for energy are typically much smaller than the energy time constants, so that the implicit correction represented by this term is very small. Secondly, this assumption says physically that the change in the fraction of vapor crossing the interface is approximated by the change in the upstream node which seems reasonable. A final pragmatic argument is that stability can be guaranteed only if the change in the interface energy is weighted towards the upstream node.

The Flow Equation

The flow equation will be developed by combining the conservation-of-mass equation, often termed the continuity equation, with the conservation-of-momentum equation which, in porous media, is given by Darcy's law.

The conservation of mass is given by

$$\frac{\partial}{\partial t}(\phi\rho) = -\nabla\cdot\rho\mathbf{v} + S \tag{25}$$

where ϕ is the porosity, ρ is the fluid density, $\mathbf{v}$ is the Darcy velocity of the fluid, and S is the mass injection rate per unit volume.

The conservation of momentum is given by Darcy's law which in effect assumes that the momentum of the fluid can be ignored. Darcy's law is then only a force balance. It is given as

$$\mathbf{v} = -\frac{K}{\mu}(\nabla P - \rho\mathbf{g}) \tag{26}$$

where K is the intrinsic permeability, μ is the fluid viscosity, P is the fluid pressure, and $\mathbf{g}$ is the acceleration due to gravity.

Equation (26) can be substituted into (25), yielding

$$\frac{\partial}{\partial t}(\phi\rho) = \nabla\cdot\left[\frac{K}{\mu}(\nabla P - \rho\mathbf{g})\right] + S. \tag{27}$$

Integrating this equation over the volume, we have

$$\int_V \left[\frac{\partial}{\partial t}(\phi\rho)\right] dv = \oint_A \left[\frac{K}{\mu}\rho(\nabla P - \rho\mathbf{g})\cdot\hat{n}\right] da + \int_V S\,dv. \tag{28}$$

If we assume that the left-hand side of Equation (28) can be represented by an average value times the region volume, and the right-hand side can be represented by an average value over each of the m surface subsections, we have

$$V\left[\frac{\partial}{\partial t}(\phi\rho)\right] = \sum_m \left[\frac{K}{\mu}\rho(\nabla P - \rho\mathbf{g})\cdot\hat{n}\right]_m A_m + SV. \quad (29)$$

For a two-phase fluid, we have separate Darcy equations for vapor and liquid. The mobilities of each phase are highly nonlinear.

Darcy's law for each phase is given by

$$\mathbf{v}_v = -M_v[\nabla P - \rho_v\mathbf{g}] \quad (30)$$

$$\mathbf{v}_l = -M_l[\nabla P - \rho_l\mathbf{g}] \quad (31)$$

where the mobilities are defined as:

$$M_v = \frac{K}{\mu_v}R_v \quad (32)$$

$$M_l = \frac{K}{\mu_l}R_l \quad (33)$$

where R_v is the vapor relative permeability and R_l is the liquid relative permeability.

In general, the intrinsic permeability for each phase is the same, but this is not an essential assumption for the derivation or solution method.

The corresponding mass fluxes are

$$\mathbf{F}_v = \rho_v\mathbf{v}_v = -M_v\rho_v(\nabla P - \rho_v\mathbf{g}) \quad (34)$$

$$\mathbf{F}_l = \rho_l\mathbf{v}_l = -M_l\rho_l(\nabla P - \rho_l\mathbf{g}). \quad (35)$$

The total flux is

$$\mathbf{F} = \mathbf{F}_v + \mathbf{F}_l = -(M_v\rho_v + M_l\rho_l)\nabla P + (M_v\rho_v^2 + M_l\rho_l^2)\mathbf{g}. \quad (36)$$

We will substitute this fluid flux for $\rho\mathbf{v}$ in Equation (25). We can justify doing this rather than writing separate mass conservation equations for each phase because the total amount of each phase is not being conserved, but only the total amount of fluid. We must, however, know what fraction of the flux is vapor to properly compute the conservation of energy as we have shown. We are implicitly assuming that the two phases are in thermodynamic equilibrium. This means that the characteristic time for the equilibrium process between phases in a given node is small compared to the typical time step used in modelling the system numerically. We feel intuitively that this characteristic time is small, but this assumption may perhaps be incorrect under some conditions.

Following the suggestion of S. K. Garg (personal comm., 1974), we can write a combined form of the fluid flow equation:

$$\mathbf{F} = -(M\rho)^*\nabla P + (M\rho^2)^*\mathbf{g} \quad (37)$$

where $(M\rho)^* = M_v\rho_v + M_l\rho_l$ and $(M\rho^2)^* = M_v\rho_v^2 + M_l\rho_l^2$.

The two-phase flow equation corresponding to the single-phase flow Equation (29) can therefore be written:

$$V\left[\frac{\partial}{\partial t}(\phi\rho)\right] = \sum_m [(M\rho)^*\nabla P\cdot\hat{n} - (M\rho^2)^*\mathbf{g}\cdot\hat{n}]_m A_m + SV. \quad (38)$$

Difference Form of Flow Equation

Both the one- and two-phase flow equations can be written in the form of the two-phase flow equation given as Equation (38). Using the general numerical method developed in the section above, we can write the corresponding difference equation for Equation (38) as

$$\left(\phi + \rho\frac{\partial\phi}{\partial\rho}\right)_n V_n \frac{\Delta\rho_n}{\Delta t} = \sum_m A_{n,m}\left[(M\rho)^*_{n,m}\left(\frac{P_m - P_n}{D_{n,m}}\right) - (M\rho^2)^*_{n,m}\beta_{n,m}g\right] + S_n V_n \quad (39)$$

where $\beta_{n,m}$ is the direction cosine between the normal from node n to m and the gravitational acceleration vector.

The complete difference equation can now be written:

$$\left(\phi + \rho\frac{\partial\phi}{\partial\rho}\right)_n V_n \frac{\Delta\rho_n}{\Delta t} = \sum_m A_{n,m}\left[(M\rho)^*_{n,m}\left(\frac{P_m - P_n}{D_{n,m}}\right) - (M\rho^2)^*_{n,m}\beta_{n,m}g\right] + \theta\sum_m A_{n,m}\left\{\left[X_{n,m}\frac{d_{m,n}}{D_{n,m}} - \frac{(M\rho)^*_{n,m}}{D_{n,m}}\frac{\partial P_n}{\partial\rho_n}\right]\Delta\rho_n + \left[X_{n,m}\frac{d_{n,m}}{D_{n,m}} + \frac{(M\rho)^*_{n,m}}{D_{n,m}}\frac{\partial P_m}{\partial\rho_m}\right]\Delta\rho_m\right\} + S_n V_n \quad (40)$$

where

$$X_{n,m} = \left(\frac{\partial(M\rho)^*}{\partial\rho}\right)_{n,m}\left(\frac{P_m - P_n}{D_{n,m}}\right) - \left(\frac{\partial(M\rho^2)^*}{\partial\rho}\right)_{n,m}\beta_{n,m}g$$

$$(M\rho)^*_{n,m} = \frac{D_{n,m}(M\rho)^*_n(M\rho)^*_m}{d_{n,m}(M\rho)^*_m + d_{m,n}(M\rho)^*_n}$$

$$(M\rho^2)^*_{n,m} = \frac{(M\rho^2)^*_n(M\rho)^*_m d_{n,m} + (M\rho^2)^*_m(M\rho)^*_n d_{m,n}}{d_{n,m}(M\rho)^*_m + d_{m,n}(M\rho)^*_n}.$$

The values of $(M\rho)^*_{n,m}$ and $(M\rho^2)^*_{n,m}$ have been derived in terms of the values in nodes n and m in order to guarantee the continuity of fluid flux and pressure at the interface.

We have now developed the flow difference equation which is solved together with the energy difference equation by the SHAFT program.

EXAMPLES OF RESULTS

To illustrate some capabilities of the SHAFT program, preliminary results from two two-phase geothermal reservoir simulations will be given. Examples of one-phase problems solved by use of an earlier version of SHAFT have already been discussed by Lasseter and Witherspoon (1974). The results described here demonstrate the application of the program to liquid-dominated and vapor-dominated geothermal systems. While these examples are similar in some

Table 2. Assumed reservoir properties.

Porosity	0.2
Permeability	5.0 millidarcies
Fluid conductivity	0.65 J/m·°C·sec
Solid conductivity	2.18 J/m·°C·sec
Solid heat capacity	1000 J/kg·°C
Solid density	2.5 g/cm³

respects to existing geothermal systems, they are intended primarily as demonstrations of the program's capabilities and no attempt has been made to model actual field behavior.

Liquid-Dominated System

For a liquid-dominated system, we have selected an axisymmetric model 2000 m high and 5000 m in radius. The zoning consists of 10 evenly spaced vertical nodes and 25 evenly spaced horizontal nodes. Hot water at a temperature of 250°C is upwelling into the bottom node on the axis at a rate of 100 tons per day. The bottom boundary is otherwise a no-flow boundary held at a constant temperature of 100°C. The top boundary is permeable and adiabatic with the pressure at the boundary being held at 1 kg/cm². The other boundaries have no flow of heat or fluid across them. The constant material properties are given in Table 2. Input tables give the internal energy, density, viscosity, and phase of the fluid as a function of temperature and pressure. Relative permeability values are tabulated as a function of volumetric vapor saturation.

For simplicity, the problem was started with a uniform temperature and pressure everywhere and was allowed to run until a steady state was reached. This necessitated running the problem for approximately one million days of physical time, which required about 100 seconds of computer time. The temperature, density, and flow fields are shown in Figure 2.

Having established the steady-state flow field, field production was simulated by withdrawing fluid from the node on the axis at a depth of 700 m at a daily rate of 100 tons (4167 kg/hr). The flow field under these conditions after 20 years is shown in Figure 2D. We see that the flow is no longer moving to the surface as before, but now is directed towards the well. The temperature and density distributions are not appreciably changed from their initial values, even after 20 years. It was thought that some phase change might occur by this time, but this did not happen. It is possible that with a higher bottom-boundary temperature and with finer zones near the well some phase transitions will develop.

Vapor-Dominated System

To study a vapor-dominated system, a model based loosely on The Geysers field was selected. The model consists of an axisymmetric system 2000 m in radius and 3000 m high. The zoning consists of 15 evenly spaced nodes in the vertical direction and 10 nodes in the horizontal direction whose spacing increases with radius. The same material properties as given in Table 1 were used except that the permeability is 1 darcy and the system is almost completely filled with steam. The bottom boundary is a no-fluid-flow boundary

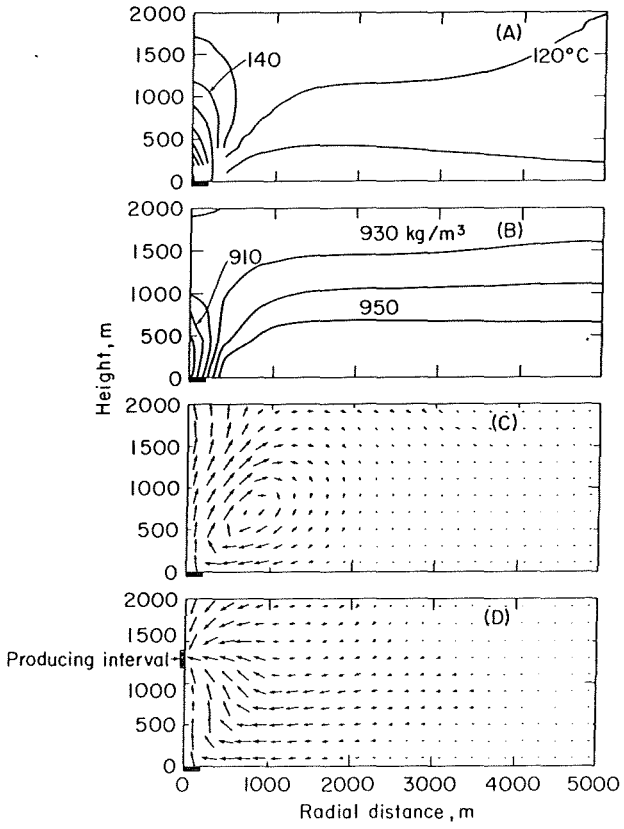

Figure 2. Liquid-dominated system showing (A) temperature field, (B) density field, (C) mass flux for initial steady state conditions, and (D) mass flux after 20 years of production.

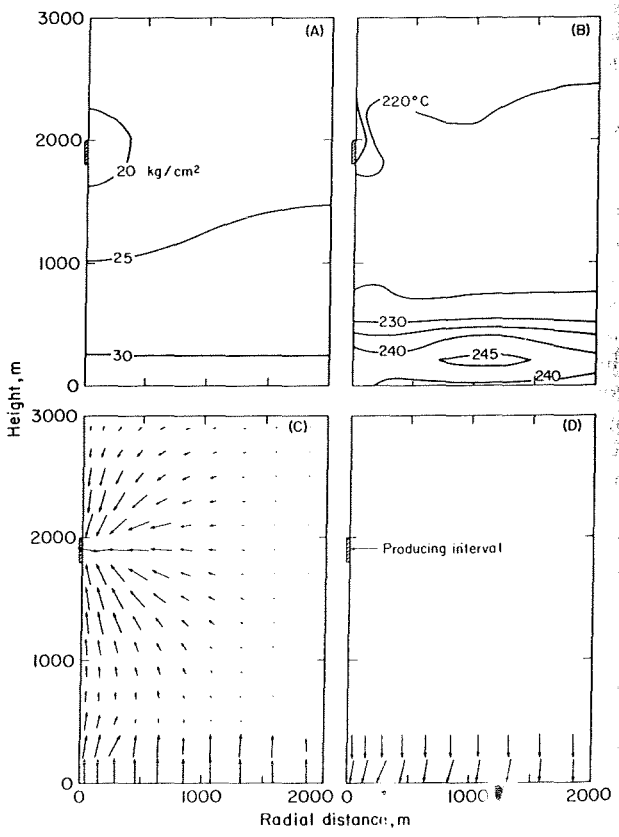

Figure 3. Vapor-dominated system showing reservoir conditions after 1500 days of production: (A) pressure field, (B) temperature field, (C) vapor flux, (D) liquid flux.

fixed at a temperature of 250°C. The other boundaries have no flow of heat or fluid across them. Steam is being withdrawn from the three nodes nearest the axis at a depth of 1100 m at a total rate of 3×10^4 ton/day (1.25×10^6 kg/hr). This flow rate is probably unreasonably high, but was selected to examine the problem of total system depletion and the effect on a boiling layer of water that was assumed to exist in the bottom 200 m of the vertical column. The system begins at a temperature of 250°C and an average pressure of 35 kg/cm^2.

Plots of temperature, pressure, liquid flux, and vapor flux after 1500 days of production are shown in Figure 3. The boiling at the bottom of the system is clearly seen from the vector plots (Fig. 3 C and D). As the steam rises, the liquid moves downward to replace it. The average system temperature decreased to about 225°C and the mean pressure of the steam column decreased to about 25 kg/cm^2. Vapor-dominated systems usually remain isothermal, and we suspect that the input convergence criterion for this problem was not adequate. We are currently investigating this.

ACKNOWLEDGMENT

This work was performed under the auspices of the U.S. Energy Research and Development Administration.

REFERENCES CITED

Darcy, H., 1856, Les fontaines publiques de la ville de Dijon: Paris, Victor Dalmont.

Edwards, A. L., 1972, TRUMP: A computer program for transient and steady state temperature distribution in multidimensional systems: Livermore, California, Lawrence Livermore Lab. Rept. UCRL-14754, Rev. 3.

Evans, G. W., Brousseau, R. J., and Keirstead, R., 1954, Instability considerations for various difference equations derived from the diffusion equation: Livermore, California, Lawrence Livermore Lab. Rept. UCRL-4476.

Lasseter, T. J., 1975, SHAFT: A computer program for the numerical simulation of heat and mass transfer in multidimensional two-phase geothermal reservoirs: Prelim. rept. by Geonuclear Nobel Paso, Geneva, Switzerland, to the Lawrence Berkeley Lab., Berkeley, California.

Lasseter, T. J., and Witherspoon, P. A., 1974, Underground storage of liquified natural gas in cavities created by nuclear explosives: Berkeley, California, Univ. of California, Dept. of Civil Engineering, Pub. no. 74-1.

Witherspoon, P. A., Neuman, S. P., Sorey, M. L., and Lippmann, M. J., 1975, Modeling geothermal systems: Presented at the International Meeting on Geothermal Phenomena and Its Applications, Accademia Nazionale dei Lincei, Rome (Berkeley, California, Lawrence Berkeley Lab. reprint LBL-3263).